ARTICLE IN PRESS
JID: YICAR [m5G;December 16, 2016;14:42]
Icarus 000 (2016) 1–13
Contents lists available at ScienceDirect
Icarus
journal homepage: www.elsevier.com/locate/icarus

# A possibly universal red chromophore for modeling color variations on Jupiter

L.A. Sromovsky[a,*], K.H. Baines[a], P.M. Fry[a], R.W. Carlson[b]

[a] Space Science and Engineering Center, University of Wisconsin, Madison, WI 53706, United States
[b] Jet Propulsion Laboratory, California Institute of Technology, Pasadena, CA 91109, United States

ARTICLE INFO

*Article history:*
Received 8 July 2016
Revised 9 November 2016
Accepted 10 December 2016
Available online xxx

ABSTRACT

A new laboratory-generated chemical compound made from photodissociated ammonia ($NH_3$) molecules reacting with acetylene ($C_2H_2$) was suggested as a possible coloring agent for Jupiter's Great Red Spot (GRS) by Carlson et al. (2016, Icarus 274, 106–115). Baines et al. (2016, Icarus, submitted) showed that the GRS spectrum measured by the visual channels of the Cassini VIMS instrument in 2000 could be accurately fit by a cloud model in which the chromophore appeared as a physically thin layer of small particles immediately above the main cloud layer of the GRS. Here we show that the same chromophore and same layer location can also provide close matches to the short wavelength spectra of many other cloud features on Jupiter, suggesting this material may be a nearly universal chromophore that could explain the various degrees of red coloration on Jupiter. This is a robust conclusion, even for 12% changes in VIMS calibration and large uncertainties in the refractive index of the main cloud layer due to uncertain fractions of $NH_4SH$ and $NH_3$ in its cloud particles. The chromophore layer can account for color variations among north and south equatorial belts, equatorial zone, and the Great Red Spot, by varying particle size from 0.12 µm to 0.29 µm and 1-µm optical depth from 0.06 to 0.76. The total mass of the chromophore layer is much less variable, ranging from 18 to 30 µg/cm$^2$, except in the equatorial zone, where it is only 10–13 µg/cm$^2$. We also found a depression of the ammonia volume mixing ratio in the two belt regions, which averaged $0.4 - 0.5 \times 10^{-4}$ immediately below the ammonia condensation level, while the other regions averaged twice that value.



## 1. Introduction

It has long been known that the condensable molecules near the visible cloud level in Jupiter's atmosphere, including ammonia and ammonium hydrosulfide, are colorless at visible wavelengths, while Jupiter's cloud features have an overall red coloration to varying degrees, as evident from the spectral samples shown in Fig. 1. Jupiter's clouds presumably contain some unknown compound that absorbs blue light preferentially, with the Great Red Spot being a region of enhanced red coloration. A number of suggestions have been made over the years to explain the color of the GRS, including molecules involving nitrogen, sulfur, phosphorous, and various compounds generated by irradiation, and complex organics of unknown composition such as tholins, as summarized by West et al. (1986) and further reviewed by West et al. (2009). Recent arguments have been advanced for irradiated $NH_4SH$ by Loeffler et al. (2016). Until recently no accurate match to the GRS spectrum had ever been demonstrated. Judging on the basis of spectral fit quality, the most promising material suggested as the GRS coloring agent is a laboratory-generated chemical compound made from photodissociated ammonia ($NH_3$) molecules reacting with acetylene ($C_2H_2$), described by Carlson et al. (2016). Baines et al. (2016) showed that the GRS spectrum measured by the visual channels of the Cassini VIMS instrument in 2000 could be accurately fit by a cloud model in which the chromophore appeared as a physically thin layer of small chromophore particles immediately above the main cloud layer of the GRS, which they referred to as the crème brûlée model because of the dessert's analogous vertical structure. They also considered other models in which the chromophore appeared in a vertically detached stratospheric haze, which did not fit as well, or as a coating on the particles of the main cloud layer, for which the fit was significantly worse.

Here we use the same VIMS data set, but extend the analysis to other cloud features and consider more varied vertical structures, showing that models using the same chromophore can fit much of the color variation that is normally seen over Jupiter's disk.

* Corresponding author.
*E-mail address:* larry.sromovsky@ssec.wisc.edu (L.A. Sromovsky).

http://dx.doi.org/10.1016/j.icarus.2016.12.014
0019-1035/© 2016 Published by Elsevier Inc.

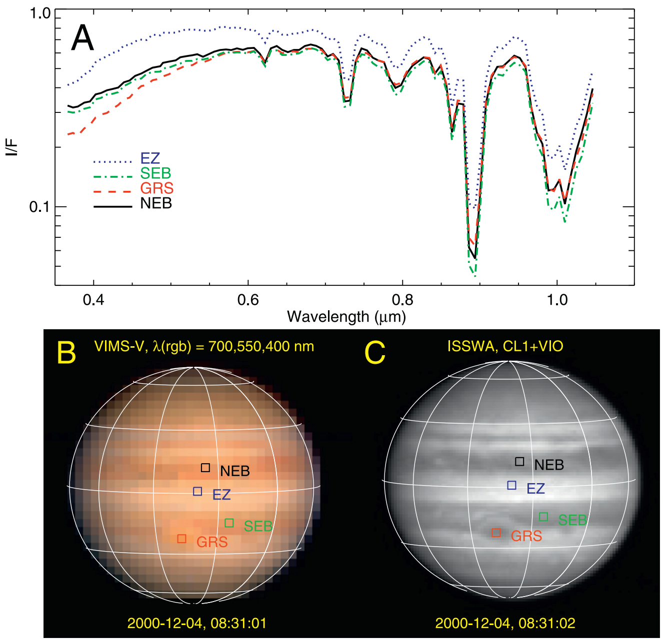


**Fig. 1.** A: VIMS spectra from locations indicated in the VIMS image composite (B) and the ISS Violet-filtered image (C). The VIMS color composite image of Jupiter on 4 December 2000 used wavelength assignments given in the legend. The corresponding ISS image is nearly simultaneous with the VIMS observation. The grids are spaced 30° in planetocentric latitude and longitude. Overplotted squares indicate locations of spectral samples used to characterize the GRS (red, dashed), SEB (green, dot-dash), EZ (blue, dotted) and NEB (black, solid). (For interpretation of the references to color in this figure legend, the reader is referred to the web version of this article.)

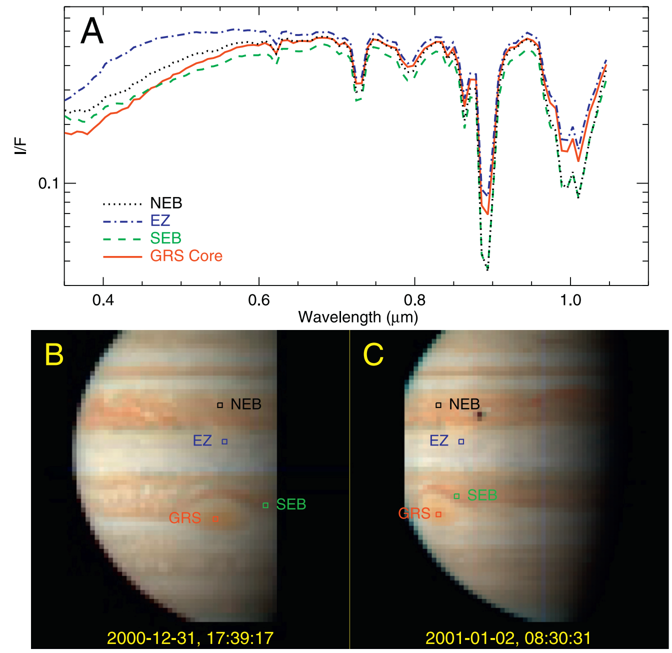


**Fig. 2.** A: spectral samples from VIMS image cube V1357116132_1 (from which the color composite in C was made). B: color composite image from VIMS cube V1356976257_3, taken when features in C were positioned closer to the terminator. The wavelengths used for blue, green, and red channels in the composite images are 450, 550, and 750 nm, respectively. The locations of spectral samples are indicated by colored squares and labels. Observation C was made 38.85 h after observation B. Samples in the second cube were acquired at positions as close as possible to the predicted locations of features shown in B, accounting for drift due to Jupiter's zonal wind profile. The dark pixel in image C (below the B in NEB) is due to the transit of Europa. (For interpretation of the references to color in this figure legend, the reader is referred to the web version of this article.)

## 2. Observations

### 2.1. VIMS instrumental characteristics

The VIMS instrument (Brown et al., 2004) provides two overlapping spectral channels covering the ranges from 0.3 to 1.05 µm (VIS) and from 0.86 to 5 µm (IR) with an effective pixel size of 0.5 milliradians on a side and a near-IR spectral resolution of approximately 15 nm (sampled at intervals of approximately 16 nm). The IR channel uses a linear detector to record a spectrum for a single spatial pixel, so that an image must be acquired by scanning the FOV across the target. The visual observations use a CCD matrix detector which records both spectral and spatial information simultaneously. The image of the target is focused on an entrance slit which is dispersed by a grating and focused on a two-dimension CCD detector array, recording spatial information along the slit direction but spectral information in the dispersion direction. In the normal mode of operation on-chip summing is used to achieve a spectral resolution of 7.3 nm and a spatial resolution of 0.5 milliradians.

### 2.2. Cassini VIMS observations of Jupiter

In December 2000, the Cassini spacecraft passed near Jupiter for a gravitational assist on its journey to Saturn. During the flyby it observed Jupiter using a suite of instruments that included VIMS, which provided spectral observations of Jupiter's atmosphere under conditions summarized in Table 1. The spatial resolution of the observations is limited by the rather large distance of the flyby. The low phase angle image acquired on 4 December is well suited for comparison with groundbased observations that provide a verification of the VIMS calibration at CCD wavelengths, but has relatively low spatial resolution. Images extracted from this data set and spectral samples at key locations can be seen in Fig. 1. The two observations at intermediate phase angles, from 31 December and 2 January, have much better spatial resolutions and provide two different observing geometries of the GRS and other cloud features, yielding additional constraints on radiative transfer models. Example images and spectral samples from these later data are provide in Fig. 2

### 2.3. VIMS calibration and navigation

The VIMS data set we used was reduced and calibrated using the USGS ISIS3 (Anderson et al., 2004) vimscal program, which was derived from the software provided by the VIMS team (and is available on PDS archive volumes), and uses the same calibration files and solar spectrum. A sanity check on the calibration was obtained by computing a disk average spectrum from the low-phase angle VIMS cube and comparing it with disk-averaged observations of Karkoschka (1998) taken in 1995 and 1993. The results, shown in Fig. 3, are plausibly consistent within 10%, given the time difference between the two observations sets. A more contemporaneous calibration check is provided by Cassini ISS band-pass filtered images of the type shown in Fig. 1B, which provide comparisons at discrete wavelength bands, as shown in Fig. 3B. The ISS calibration leads to I/F values that are 20% greater than produced with the VIMS calibration. Given that the ISS calibration is being revised to put it into better agreement with the Karkoschka groundbased observations, we also considered Hubble Space Telescope WFPC2 observations obtained on 14 October 1999 as another sanity check. Unfortunately, most of those WFPC2 observations were overexposed, partially saturated, and not usable for disk-integrated comparisons. Three images that were not saturated